ELSEVIER

Journal of Photochemistry and Photobiology A: Chemistry 118 (1998) 151–156

Journal of Photochemistry and Photobiology A:Chemistry

Adiabatic structural relaxation in heterocyclic nitrogen-containing cations The structure, absorption and fluorescence of the 2,4,6-triarylsubstituted pyridinium cations

Michael I. Knyazhansky[1], Vladimir A. Kharlanov[*], Ya.R. Tymiansky

Institute of Physical and Organic Chemistry, Rostov State University, Stachka str. 194/2, Rostov on Don 344104, Russia

Received 6 April 1998; accepted 17 August 1998

Abstract

The detailed studies of the 2,4,6-(N-alkyl)triarylsubstituted pyridinium cations **I** as well as the large series of the model structures have been carried out by absorption, fluorescent and polarization methods in the solvents of various polarity and viscosity at different temperatures. The localizations of the lowest electron transitions are determined. It is shown that the fluorescence with anomalous Stokes shift (ASS-fluorescence) arises owing to the adiabatic structural relaxation (ASR) with the formation of the flattened (but not twisted) structure. The advantages of **I** as the objects for ASR study are discussed. The crude determination of the ASR kinetic parameters has been conducted. A data assume that the ASS fluorescence quantum yields of the cations **I** are conditioned mainly by deactivation processes in the final flattened structure.

Keywords: 2,4,6-triarylsubstituted pyridinium cations; Absorption; Adiabatic structural relaxation

1. Introduction

The first cycle of investigation of the light-induced processes in the arylsubstituted pyridinium cations was connected with the elucidation of the basic structural mechanism of the spectral-luminescent and photochemical properties in N-alkyl and N-aryl derivatives of 2,4,6-arylsubstituted cations [1]. The following series of works were devoted to the studies of the mechanisms of photocyclization in various N–R derivatives of 2,4,6-aryl substituted cations (R: aryl, amine and azomethine) [2,3]. Due to the important role of the N-aryl fragment in the formation of luminescent properties, systematic studies of the photophysical and structural relaxation processes in the various simplest N-aryl substituted cations (without 2,4,6-aryl substitutes) have been carried out by us recently [4–7].

At the same time series of crucial problems connected with the Anomalous Stokes Shift fluorescence (ASS-fluorescence) as result of adiabatic structural relaxation (ASR) in 2,4,6-triarylsubstituted pyridinium cations is studied quiet insufficiently or is not solved at all.

Especially it concerns the nature of electronic transitions responsible for cation excitation and also the influence of the molecular structure and environment on the kinetic parameters characterizing ASS fluorescence and ASR.

Thus the main objectives of this and following papers are detailed description and discussion of the experimental findings connected with the molecular structure, environment's polarity, viscosity and temperature influence on the formation of the spectro-fluorescent properties and kinetic characteristics of the ASR processes in 2,4,6-triarylsubstituted pyridine cations without N–Ar fragment.

*Corresponding author. E-mail: photo@ipoc.rnd.runnet.ru

[1]Also corresponding author.

1010-6030/98/$ – see front matter
PII: S1010-6030(98)00377-3

2. Experimental

2.1. Materials

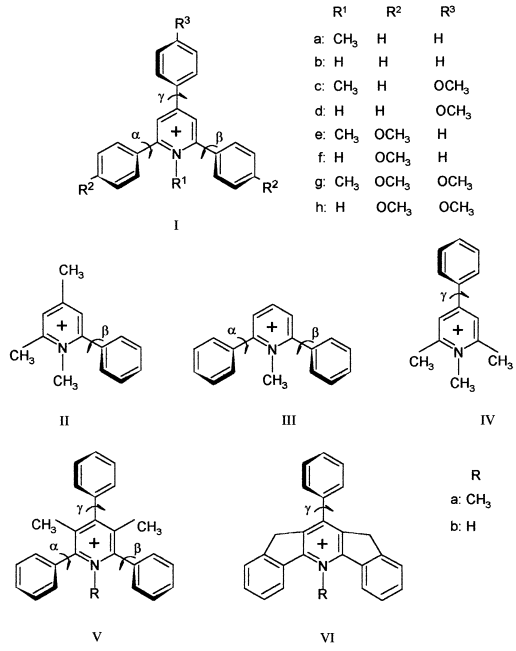

The objects of the investigations are the pyridinium cations **I** and also the main model compounds in which the influence of the different aryl rings is excluded (**II–IV**) or their various acoplanarity degrees (the angles α, β) are provided (**V**, **VI**). All pyridinium salts are used in the form of perchlorates (anion ClO_4^-). The catalytic amounts of the chlorine acid ($HClO_4$) are added in the solvents for stabilization of the cations **Ib**, **Id**, **If**, **Ih** and **Vb**, **Vb**.

Commercially available organic solvents employed in experiments were found to give no detectable fluorescence under experimental conditions.

2.2. Spectral investigations

The absorption and fluorescence steady-state spectroscopy have been used for comparative investigations of cations **I** and model compounds **II–VI**. Absorption spectra were recorded with Specord M40 and a Specord UV–VIS spectrophotometers (Germany) in the quartz cells with variable thickness.

The emission and excitation fluorescence spectra were measured with an Elumin 2 M spectrofluorometer (Russia) and corrected for instrument response.

The device with the optical cryostats for absorption and fluorescence spectra measurements at various temperatures in the region of -200 to $+30^\circ$C (to a precision of 1%) was utilized.

The fluorescence quantum yields (Φ_f) were obtained by the relative Parker–Rees method (to precision of 10%) with phenanthrene in ethanol ($\Phi_f = 0.13$ at 290 K) and 9,10-diphenylanthracene in benzene ($\Phi_f = 0.84$ at 290 K) as references [8]. The excitation fluorescence polarization spectra were registered by a Hitachi 650–60 spectrofluorometer (Japan) with film polarizers.

The measurements of fluorescence lifetime were performed with nanosecond spectrometer SP-70 (England) in Moscow State University.

3. Results and discussion

3.1. Absorption spectra and molecular structure

According to the findings of the X-ray and NMR studies obtained before [9,10] the structures **I** under study are acoplanar significantly (for **Ia** α, $\beta \approx 50$–60°, $\gamma \approx 30^\circ$, for **Ib** α, β, $\gamma \approx 30^\circ$).

The typical absorption bands (Fig. 1, Table 1) are observed with an insignificant spectral shift in the solutions of different polarity – **A** ($\lambda_{max} \approx 310$ nm) and **B** ($\lambda_{max} \approx$ 250–260 nm).

The compounds **I** are the derivatives of heteroaromatic analogs of the metapolyphenyl molecular system. Therefore to ascertain the nature of the electronic transitions in **I**, it is worthwhile to consider the absorption spectra of more simple model structures – polyphenyl derivatives of benzene, pyridine and pyridinium (Table 1).

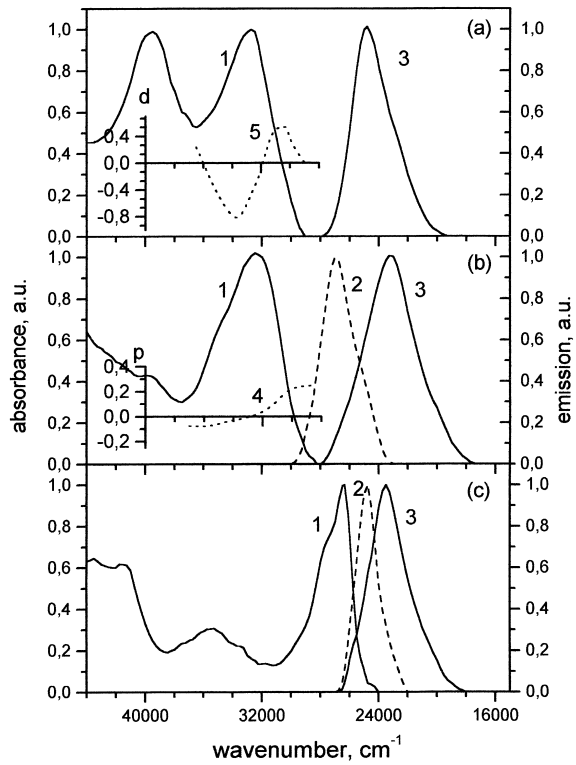

Fig. 1. The absorption 1 (ethanol, 296 K), fluorescence 2 (ethanol, 77 K) and (ethanol, 295 K), excitation polarization 4 (glycerine, 295 K) and circular dichroism 5 (ethanol, 294 K) spectra of (a) **Ia**, (b) **Ib**, (c) **VIa**.

Table 1
The absorption spectrum bands of the compounds **I–III** and the model polyphenyl derivatives of the benzene, pyridine and pyridinium (ethanol, 295 K)

Compound	A-band		B-band	
	λ_{max} (nm)	ε_{max} (l M^{-1} cm^{-1})	λ_{max} (nm)	ε_{max} (l M^{-1} cm^{-1})
Ia	32 600	40 000	40 000	16 500
Ib	32 560	22 100	39 980	22 200
Ic	28 400	35 000	41 650	20 000
Id	29 600	36 000	40 000	24 000
Ie	28 000; 29 000	17 500; 24 000	43 480	17 000
If	28 680	35 000	40 000	22 000
Ig	28 640	54 000	37 040	15 000
Ih	28 320	32 100	37 040	16 000
II	35 300	9600	40 000	2800
III	32 800	13 000	40 000	5500
Biphenyl [11]	–	–	40 000	14 000
1,3-Diphenyl benzene [11]	–	–	40 500	39 000
1,3,5-Triphenyl benzene [11]	–	–	39 700	70 000
2-Phenyl pyridine [19]	36 200	10 400	40 500	13 400
2,6-Diphenyl pyridine [19]	33 100	11 800	40 800	34 400
2,4,6-Triphenyl pyridine [19]	31 900	9000	38 900	53 500

It is known [11] that the *meta*-substituted polyphenyl compounds can be presented as the superposition of the weakly interacting biphenyl fragments. The biphenyl absorption band with $\nu_{max} = 40\,000\ cm^{-1}$ ($\gamma_{max} = 250$ nm) has been interpreted as $^1L_a - ^1A_1$ electronic transition [11]. Hence, the B-absorption band of the **Ia**, **b** compounds can be viewed as the superposition $^1L_a - ^1A_1$ transitions in each of three modified biphenyl fragments.

That each of the analogous series: benzene, pyridine and pyridinium derivatives of B-band intensity increases without considerable spectral shift is observed with the successive growth of the metaphenyl substituents' number.

Meanwhile, another clear regularity is also displayed and connected with considerable B-band intensity fall by the increase of electron acceptor ability of a ring in the biphenyl-similar fragments with a transition from benzene to pyridine and pyridinium derivatives (Table 1).

Analogous regularity is observed with the pyrilium cations [1] (i.e. with the heteroring acceptor ability increase) and also by the introduction of the electron donor substituents to the different aryl rings of the arylsubstituted pyridines and pyridiniums.

The band A playing a key role under consideration of the luminescent properties of the compounds **I** appears only in the heteroatomic analogs of the biphenyl systems. Its intensity and red shift increase as a rule with the growth of the donor and acceptor abilities of the aryl and heterorings, respectively (Table 1).

Therefore, it is natural to assume that this broad band (the half-width $\Delta\nu_{1/2} = 5200\ cm^{-1}$) is connected with intramolecular charge transfer (ICT) from both the different types of structurally unequivalent phenyl substituents (2,6 or 4) on the heteroring. With the use of the circular dichroism method it has been shown by us earlier that the A-band is the superposition of two transitions shifted relatively towards each other [1] (Fig. 1(a)).

For a detailed study of this problem the fluorescence excitation polarization spectra in A-band together with the structure modelling method are used. One can see (Fig. 1(b)) that the A-band in the compound **Ia** as above, is the superposition of two spectrally shifted transitions which are polarized differently and the polarizations of the longwave absorption and emission transitions coincide.

At same time in the model compound without 4-phenyl ring **III** the polarization degree is positive throughout the A-band width (Fig. 2(a)). Thus, it is possible to infer that the longwave transition ($\nu_{max} = 32\,000\ cm^{-1}$) in the compounds **Ia**, **b** is connected with ICT from 2,6-phenyl rings and more shortwave transitions ($\nu_{max} = 34\,000\ cm^{-1}$) is the ICT from 4-phenylsubstituent.

With the inclusion of donor substituents (p-OCH_3) in the 2,6-phenyl rings (the compounds **Ie**, **f**) the drastic red shift of the longwave ICT-transition and clear separation of the differently polarized bands are observed (Fig. 2(b)). On the other hand, the inclusion of only the p-OCH_3 group in the 4-arylsubstituted leads to the inversion of differently localized longwave transitions. Therefore, the transition localized on the 4-aryl fragment becomes the largest longwave transition. By it the A-band is again the superposition of differently polarized transitions but its shape basically changes (Fig. 2(c)). It follows, however, that the large A-band width in both studied (**Ia**, **b**) and model (**III**, **IV**) compounds ($\Delta\nu_{1/2}$=4600–5500 cm^{-1}) is indicative of the possibility of its unhomogeneous widening at the expense of rotamers' distribution at α, β, γ angles.

Actually, the drastic displacement of the rotamers' distribution to the aryl ring acoplanarity (the compound **V**) leads to a typical ICT-transition shortwave shift of the A-band ($\Delta\nu = 1500\ cm^{-1}$) with its intensity decreasing. On other hand, the 'narrowing' of the rotamers' distribution in the 'fastened' and 'flattened' model structure VI assesses marked A-band width drop ($\Delta\nu_{1/2} = 2600\ cm^{-1}$)

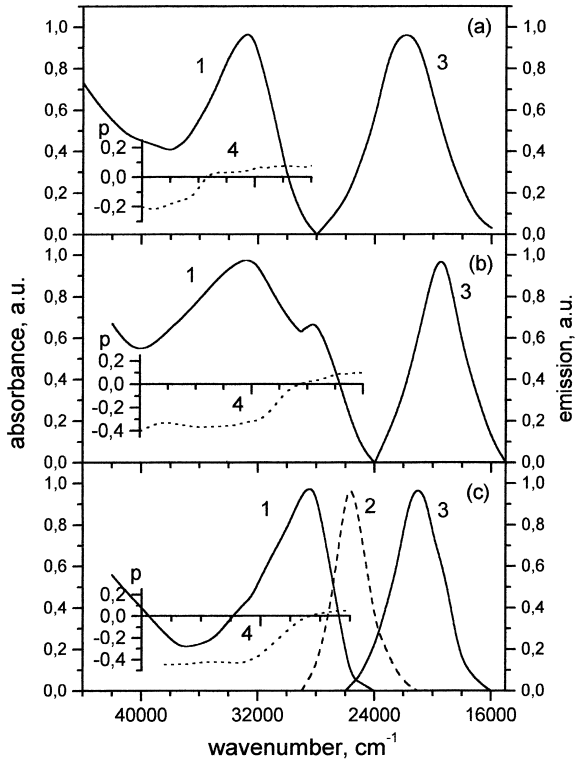

Fig. 2. The absorption 1 (ethanol, 296 K), fluorescence 2 (ethanol, 77 K) and 3 (ethanol, 295 K) and excitation polarization 4 (glycerine K) spectra of (a) **III**, (b) **Ie**, (c) **Ic**.

(Fig. 1(c)). Thus, the above described experimental results may be summarized as follows:

1. The B-band in the cations **Ia**, **b** are the superposition of the three weakly interacting *meta*-biphenyl fragments.
2. The A-band is the superposition of two differently localized electronic transitions connected with ICT onto the positive-charged heteroring from 4-aryl (the shortwave transition) and 2,6-aryls (the longwave transition). The significant A-band unhomogeneous widening is explained by rotamers' distribution by α, β, γ angles in the ground state.
3. The interaction is realized between differently localized biphenyl (the band B) and ICT (the band A) transitions leading to antibate changes of their intensities.

3.2. Fluorescence with anomalous Stokes shift and structural relaxation in the liquid solvents

On excitation into the longwave absorption band A the longwave intensive ASS-fluorescence of **Ia**–**Ic** arises in the various solvents at the room temperature (Table 2, Fig. 1(a)–(c)). The fluorescence quantum yield dependence on concentration (10^{-6}–10^{-3} M) is absent and therefore the eximers cannot be responsible for ASS-fluorescence.

On other hand, the influence of solvent polarity (from chloroform with $\varepsilon = 4.8$ till DMSO with $\varepsilon = 48.9$) on the fluorescence band position is insignificant and this is the consequence of the lack of dipole–dipole interaction of the solute–solvent system owing to the ionic structure of the studied compounds [12].

The advantage of such ionic structures is one of the important causes for the choice of the compound **I** as the object for investigations.

Thus, the above-mentioned findings are indicative of the intramolecular nature of ASS-fluorescence, which is connected with the adiabatic molecular structure changes in $\mathbf{S}_1$-state due to the excitation of the initial structure **I** (ASR).

Such structural transformation in the compounds **I** may be connected with a rotation of the 2,4,6-aryl rings about C–C bonds (angles α, β, γ). At same time the basic role in compounds **Ia**, **Ib** is played by rotation of the 2,6-rings (angles α, β). This can be seen from the comparison of the Stokes shift of **Ia**, **Ib** and model compounds **II**, **III** (Table 2).

In this case the hindrances in the 2,6-rings' rotation in the viscous (or rigid) environment lead to a drastic decrease of

Table 2
The fluorescence (the fluorescence quantum yield Φ_{rf}^0 and decay τ_f) of the compounds **I–VI**

Compound	ν_{max}^f (cm^{-1}) (λ_{max}^f, nm) Ethanol, 295 K	$\Delta\nu_{a-f}$ (cm^{-1}) Ethanol, 295 K (glycerin, 295 K)	Φ_{rf}^0 Ethanol, 295 K	τ_f (ns) Ethanol, 295 K
Ia	22 800 (439)	9800 (8100)	0.32	1.85
Ib	24 700 (405)	7900	0.37	1.00
Ic	21 050 (475)	7350 (6500)	0.23	1.30
Id	21 730 (460)	7870	0.29	1.30
Ie	19 320 (518)	8680 (7800)	0.95	5.30
If	21 320 (469)	5710	0.86	4.20
Ig	19 510 (513)	9130 (8200)	0.56	4.35
Ih	22 400 (446)	6200	0.94	–
II	26 880 (372)	8680	–	–
III	21 730 (460)	11 150 (9320)	0.10	0.82
IV	27 780 (360)	6820	–	–
Va	25 180 (397)	9220	–	–
Vb	25 770 (388)	7930	–	–
VIa	23 500 (426)	2800	0.85	–
VIb	24 700 (405)	3500	0.85	–

the Stokes shift. It is observed in the glassy solvent (77 K) (Fig. 1(a) and (b)) and testifies to the offered ASR mechanism. Such a simple ASR mechanism and its distinct manifestation in fluorescence properties are the important characteristics of the cations I which also favour their use as objects for ASR studies.

In this situation the problem of the ASR direction acquires principal importance. As is well known ICT transition may be followed by the ASR process connected mainly with the aryl ring orthogonalization leading to the TICT-like or local fluorescent state formation [13–16]. On the other hand, the flattened fluorescent structure formation may occur only upon the $\mathbf{S}_0$–$\mathbf{S}_1$ excitation without ICT as for instance, in the biphenyl systems [17]. However, in our case the second path occurs in spite of the typical ICT nature of the $\mathbf{S}_0$–$\mathbf{S}_1$ excitation.

The following experimental findings testify to the latter,

1. The Stokes shift $\Delta\nu_f$ increases strongly in the series of the 2,4,6 3-phenylsubstituted pyrilium ($\Delta\nu_f = 3630\ cm^{-1}$, $\alpha = 10^\circ$), pyridine ($\Delta\nu_f = 4200\ cm^{-1}$, $\alpha = 30^\circ$), NH-pyridinium **Ib** ($\Delta\nu_f = 7900\ cm^{-1}$, $\alpha > 30^\circ$), NMe-pyridinium **Ia** ($\Delta\nu_f$ 9800 cm^{-1}, $\alpha = 65^\circ$) i.e. with a growing difference between the initial (Frank–Condon, angles α, β) and the ultimate (flattened, fluorescent) structures.
2. By the same reason the fluorescence band of the strongly acoplanar (in both $\mathbf{S}_0$ and $\mathbf{S}_1$ states) model structure **Va** is shifted to the short wavelength in comparison with **Ia** although it also has a large Stokes shift (Table 2).
3. It is shown for the cations **Ia** (earlier) [1] and **Ib** (in the present) work that the ASS fluorescence spectra of these cations are modeled sufficiently well by the rigid flattened (but not plane absolutely, α=10–15°) structure **VIa** and **VIb**, respectively (Table 2, Fig. 1(c)). The unusual ASR behaviour connected with a flattening but not with orthogonalization of the electron donor and acceptor fragments arouses significant interest.

This is an additional reason for the choice of the compounds **I** as the favourable objects for ASR studies.

Thus the fluorescence properties of the cations **I** are conditioned directly by the ASR and may be used for the study of the ASR mechanism and kinetic peculiarities and also the structure and environment influence on structural transformations.

As has been shown by virtue of the findings of the fluorescence dependence on the solvent viscosity the ASR may be considered as a continuous process on the $\mathbf{S}_1$-state surface without intrinsic barriers [18].

Such a process proceeds from the initial Frank–Condon state promoted by $\mathbf{S}_0 \rightarrow \mathbf{S}_1$ excitation ($E^{FC} = V_a^i$) till fluorescent state ($E^{Fl} = \nu_f$). The latter for **Ia**, **Ib** in the low liquid viscous solvents is connected with the flattened equilibrium conformation ($\alpha = \alpha_0 \approx 0$, $\nu_f = \nu_{eq}$) which corresponds to the model structures **VIa** and **VIb**, respectively.

Table 3
The kinetic characteristics of ARS (the rough estimation)

Cation	Ethanol, 295 K		Glycerine, 295 K	
	$k_r^0 \times 10^{-10} c^{-1}$	Φ_r^0	$k_r^0 \times 10^{-8} c^{-1}$	Φ_r^0
Ia	>5	0.38	1.1	–
Ib	>10	0.44	–	–
Ic	–	–	1.0	–
Ie	–	–	0.2	–
Ig	–	–	0.3	–
III	–	–	2.5	–

The quantum efficiencies of this structure formation (Φ_r^0) may be estimated from the values of experimentally obtained fluorescence quantum yields of the structures **Ia**, **Ib** (Φ_{rf}^0) and **VIa**, **VIb** (Φ_f^0): $\Phi_r^0 = \Phi_{rf}^0/\Phi_f^0$ (Table 3). One can assume that the electron transition energy $\Delta E_{S1-S0} = E^{FC} - E^{Fl} = \nu_a^i - \nu_f$ depends linearly on the torsional angle α:

$$\nu_f = \nu_f^i - (\nu_f^i - \nu_{eq}) \cdot \frac{\alpha - \alpha_1}{\alpha_i - \alpha_o} \quad (1)$$

where, α, α_i, α_o ($\alpha_o < \alpha < \alpha_i$) and ν_f, ν_f^i, ν_{eq} are the torsional angles and fluorescence band maxima for arbitrary, initial and flattened structures, respectively and one may to put $\nu_f^i = \nu_a^i$ where, ν_a^i is the absorption band maximum of the initial structure **I**.

As it is easy to see that at $\alpha = \alpha_i$ (the structure is not changed) $\nu_f = \nu_f^i = \nu_a^i$ and Stokes shift $\Delta\nu = 0$; at $\alpha = \alpha_o$ (after maximum flattening) the Stokes shift reaches a maximum value $\Delta\nu_f^0$. One can assume that the arbitrary change of the angle ($\alpha_i - \alpha$) with the formation of the final fluorescent structure (with angle α) corresponding to the viscosity of the given solvent is proportional to the efficiency of ASR ($\Phi_r \sim (\alpha_i - \alpha)/(\alpha_i - \alpha)$) and from (Eq. (1)):

$$\nu_f = \nu_f^i - (\nu_f^i - \nu_{eq}) \cdot \Phi_r = \nu_f^i - (\nu_f^i - \nu_{eq}) \cdot \frac{k_r}{K_r + K_d + K_f}$$

$$\Delta\nu_f = \Delta\nu_f^0 \cdot \frac{K_r}{K_r + K_d + K_f} \quad (2)$$

where $\Delta\nu_f$ is the Stokes shift under experimental conditions and k_r, k_d, k_f are the rate constants of the ASR, radiationless and emission deactivations, respectively, in the region of the conformation corresponding to α angle.

It is obvious that if $k_r^0 = 0$ (the ASR does not proceed) than $\nu_f = \nu_f^i$ and if $k_f \gg k_d + k_f$ (the ASR proceeds till the angle $a \geq a_o$) then $\nu_f \approx \nu_{eq}$ where ν_{eq} is the fluorescence band maximum of the flattened structure which is formed under excitation of **Ia**, **Ib** followed by ASR in the low viscous solvent and therefore modeled well by the structure **VIa** and **VIb** (Table 2).

It follows from the above and the experimental findings (Tables 2 and 3) that for both compounds the ASR rate constants in ethanol at the ambient temperature $k_r^0 \geq 10^{10}\ s^{-1}$ and both the efficiency and the rate of ASR are somewhat larger for the more flattened structure **Ib** (Table 3).

The attempt of direct ASR rate constant determination by the ASS-fluorescence rise time measurement with the impulse method did not allow the exact results to be obtained because of insufficiently high time resolution of the measuring device. But the findings obtained conform with the above estimation ($k_r^0 > 6\times10^{10}\ s^{-1}$).

The empirical Eq. (2) also allows estimation of roughly the k_r value molecular structure dependence by utilization of the viscous solvent at room temperature ($k_r < k_d + k_f \approx 10^{10}\ s^{-1}$) even when the model flattened structure could not synthesized. Such an estimation can be conducted by the expression (Eq. (3)) derived from (Eq. (2)):

$$k_r = \frac{\Delta\nu_f^0 - \Delta\nu_f}{\tau_f \cdot \Delta\nu_f} \quad (3)$$

where $\Delta\nu_f^0$ is the maximum Stokes shift in the low viscous media when the ultimate structure is modeled well by the flattened structure **VI** and $\Delta\nu_f$ is the maximum Stokes shift in the viscous solvent (e.g. glycerine), $\tau_f = 1/(k_d + k_f)$ is the fluorescence lifetime which is supposed to depend slightly on temperature and viscosity (as compared with k_r). The findings are provided in Table 3 for some N–CH_3 cations. One can see that k_r is lesser (on the two order of magnitude) in glycerine than in ethanol. Therefore, using the formula (Eq. (3)) we can observe a marked decrease, or on the contrary, the increase of k_r with the introduction of the donor substituents in the 2,6-aryl (the compounds **Ie** and **Ig**) or by exception of the 4-aryl ring (compound **III**), respectively (Table 3).

On the other hand, the ASR fluorescence quantum yields of the cation **I** ($\Phi_{rf}^0 = \Phi_r^0 \times \Phi_f^0$) are steeply enhanced by the inclusion of (OCH_3) substituents in the 2,6-aryl rings (the compounds **Ie**, **If**, **Ig**, **Ih**) (Table 2). Hence, the inclusion of the bulky electron donor substituents (OCH_3) leads to the decrease of ASR efficiency (Φ_r^0) but increases strongly the fluorescence efficiency of the flattened structure (Φ_f^0) at the expense of the radiationless rate decrease. The marked rise of the τ_f (at 2–3 times) can be indicative of the latter. On the other hand, the drastic fall of the fluorescence quantum yield of the cation **III** may be explained by increase of the radiationless deactivation rate in the ultimate flattened structure (τ_f (**III**) / τ_f (**I**) ≈ 0.5).

Therefore the ASS fluorescence quantum yield of the cation **I** is conditioned mainly by the deactivation processes in the final flattened structure but they are not caused by the ASR rate.

The additional quantum – chemical and direct kinetic investigation are necessary for the explanation and coordinated interpretation of these experimental data.

Acknowledgements

The authors are grateful to the International Association for Promotion of Cooperation with Scientists from the New Independent states of the Former Soviet Union (INTAS, project 96-1485) and to Prof. Dr. B. Uzhinov and Dr. S. Druzhinin (Moscow State University) for participation in the fluorescence lifetime measurements.

References

[1] M.I. Knyazhansky, Ya.R. Tymyansky, V.M. Feigelman, Heterocycles 26 (1987) 2963.
[2] V.M. Feigelman, Ya.R. Tymynskii, N.I. Makarova, M.I. Knyazhanskii, J. Phys. Organic Chem. 3 (1990) 200.
[3] Ya.R. Tymynskii, V.M. Feigelman, N.I. Makarova, M.I. Knyazhanskii, V.A. Kharlanov, V.S. Orekhovskii, M.P. Zhdanova, E.A. Zvezdina, J. Photochem. Photobiol., A: Chemistry 54 (1990) 91.
[4] V.A. Kharlanov, M.I. Knyazhansky, N.I. Makarova, V.A. Lokshin, J. Photochem. Photobiol. A: Chem. 70 (1993) 223.
[5] V.A. Kharlanov, W. Rettig, M.I. Knyazhansky, N.I. Makarova, J. Photochem. Photobiol. A: Chem. 103 (1997) 45.
[6] V.A. Kharlanov, W. Rettig, M.I. Knyazhansky, J. Mol. Struct. 380 (1996) 113.
[7] V.A. Kharlanov, W. Rettig, unpublished results.
[8] C.A. Parker, Photoluminescence of Solutions, Elsevier, Amsterdam/London/New York, 1968, p. 510.
[9] S.M. Aldoshin, Ya.R. Tymyansky, O.A. Diachenko, M.I. Knyazhansky, L.O. Atovmian, lzv. ANSSSR, ser. chem. (1981) 2270.
[10] R.M. Claramunt, F. Elguero, Coll. Czechoslovak. Chem. Commun. 46 (1981) 584.
[11] E.S. Stern, C.J. Timmons, Electronic Absorption Spectroscopy in Organic Chemistry, 3rd ed., Edward Arnold, London 1970.
[12] N.G. Bakhshiev, The Spectroscopy of the Intermolecular Interaction, Nauka, Leningrad, 1972, p. 263.
[13] W. Rettig, Top. Curr. Chem. 169 (1994) 254.
[14] W. Rettig, Angew. Chem. 98 (1986) 969.
[15] W. Rettig, Angew. Chemie Int. Ed. Engl. 25 (1986) 971.
[16] W. Rettig, V.A. Kharlanov, M. Maus, unpublished results.
[17] J.B. Berlman, J. Phys. Chem. 74 (1970) 3085.
[18] V.A. Kharlanov, Ya.R. Tymyansky, M.I. Knyazhansky, Optica and Spectrosc. 58 (1985) 1147.
[19] L. Sobszyk, Bull. Acad. Pol. Sci. 49 (1961) 237.